

## A statistical model for the determination of the optimal metric in factor analysis of medical image sequences (FAMIS)

H Benali, I Buvat, F Frouin, J P Bazin and R Di Paola  
U66 INSERM, Institut Gustave Roussy, 94805 Villejuif, France

Received 15 January 1993, in final form 19 April 1993

**Abstract.** A statistical model is added to the conventional physical model underlying factor analysis of medical image sequences (FAMIS). It allows a derivation of the optimal metric to be used for the orthogonal decomposition involved in FAMIS. The oblique analysis of FAMIS is extended to take this optimal metric into account. The case of scintigraphic image sequences is used. We derive in this case that the optimal decomposition is obtained by correspondence analysis. A scintigraphic dynamic study illustrates the practical consequences of the use of the optimal metric in FAMIS.

### 1. Introduction

Factor analysis of medical image sequences (FAMIS) is recognized as a powerful tool for extracting, in a condensed manner, functional or spectral information from dynamic or spectral image sequences (Houston 1990). As different methods have been proposed that do not yield the same results (see, for instance, Barber 1980, Bazin *et al* 1980, Di Paola *et al* 1982, Nijran and Barber 1986, Samal *et al* 1987,...), it is often considered that FAMIS has no sound foundations. This prevents FAMIS from being largely distributed and used in clinical studies. Consequently, we have undertaken to look into the theoretical basis of FAMIS.

FAMIS is based on a linear additive model, which assumes that the studied image sequence can be resolved into a limited number of fundamental spatial distributions such that the signal variation within each distribution is homogeneous. The aim of FAMIS is to estimate the underlying fundamental spatial distributions by factor images and the associated so-called fundamental functions (describing the signal variations) by factors. To perform such a decomposition, FAMIS includes four stages:

(i) Data preprocessing to improve the signal to noise ratio. This consists of a clustering and a thresholding of the set of trixels associated with the image sequence, one trixel being defined as the signal variation within one pixel or one cluster of pixels.

(ii) Orthogonal analysis of the resulting trixels. The goal of this orthogonal analysis is to determine a low-dimensional subspace, also called the 'study subspace' (Barber and Nijran 1982), in which mainly the relevant part of the trixels is represented, without the noise.

(iii) Oblique rotation of the basis vectors of the study subspace to obtain non-orthogonal basis vectors, namely the factors, having a physical or physiological meaning. This stage is called oblique analysis.

(iv) Computation of the factor images in the initial spatial sampling using an oblique projection (Di Paola *et al* 1982).

Up to now, no particular attention was paid to the choice of the metric to be used in the orthogonal and oblique analyses. Different data normalizations were proposed without any theoretical justification (Di Paola *et al* 1976, Barber 1980, Bazin *et al* 1980, Di Paola *et al* 1982, Nijran and Barber 1986, Samal *et al* 1987, Nijran and Barber 1988, Gagnon *et al* 1989, Nakamura *et al* 1989).

The optimal normalization requires the introduction of a statistical model for the medical image sequences. The solution of this statistical model leads to the expression of the optimal metric which determines the normalization of the data to be used for orthogonal analysis. In order to preserve the optimal metric for the oblique analysis, a generalization of oblique analysis is presented. Though FAMIS has been applied to various modalities of functional imaging (Frouin *et al* 1992), it is primarily used in nuclear medicine. The case of scintigraphic data is detailed and the corresponding optimal metric is deduced. The practical consequences of the use of the optimal metric compared with a conventional one are illustrated using a dynamic scintigraphic image sequence.

The importance of adding a statistical model to the conventional FAMIS model and the relevance of the proposed statistical model are discussed.

## 2. Conventional FAMIS model

A sequence of  $P$  images can be considered as a set of vectors  $x_i$  ( $i = 1 \dots N$ ) of  $P$  components  $x_{ij}$  ( $j = 1 \dots P$ ).  $x_i$  is called a trixel and represents the variation of the signal within a pixel  $i$  or a cluster  $i$  of pixels in the image sequence indexed by the variable  $j$ . Let  $y_i$  be a  $P$ -dimensional vector obtained from a transformation  $g$  of  $x_i$ :

$$y_i = g(x_i).$$

The conventional FAMIS model is based on the following hypothesis (Barber 1980, Di Paola *et al* 1982):

$$y_i = \tilde{y}_i + \epsilon_i = \sum_{k=1}^K a_k(i) f_k + \epsilon_i \quad \forall i \quad (1)$$

with

$$\sum_{j=1}^P f_k(j) = \sum_{j=1}^P y_i(j) = 1 \quad (2)$$

i.e.

$$\mathbf{F} \mathbf{1}_P = \mathbf{1}_K \quad (3)$$

where  $\mathbf{F}$  is the  $(K, P)$  matrix composed of the fundamental functions  $f_k$ ,  $\mathbf{1}_P$  is a  $(P, 1)$  matrix of ones and  $\mathbf{1}_K$  is a  $(K, 1)$  matrix of ones.  $a_k$  and  $f_k$  are the underlying fundamental spatial distributions and fundamental functions, respectively. A set  $\{a_k, f_k\}$  is called a fundamental structure.

According to this model, the relevant part  $\tilde{y}_i$  of each transformed trixel  $y_i$  can be decomposed on a basis constituted by a limited number  $K$  of fundamental functions  $f_k$

having a physical or physiological meaning. This model is mainly a physical model. It does not assume any statistical properties related to the trixel  $y_i$  or to the error  $\epsilon_i$ .

Different normalizations  $g$  of the trixels have thus been considered without theoretical foundation. The principal component analysis of the normalized data does not ensure the best separation between signal and noise since no information about the statistical properties of signal and noise is taken into account. It only provides an orthogonal decomposition of the covariance matrix of the normalized data. To achieve an optimal separation between signal and noise, their statistical properties must be considered and the only way to do this is to introduce a statistical model.

Consequently, in our approach the conventional FAMIS model is split up into a statistical model and a physical one.

### 3. A statistical model for FAMIS: the fixed-effect model

A statistical model can be applied to the data if they satisfy all the hypotheses of this model. The transformation  $g(x_i) = y_i$  of the trixels aims at transforming the data to make the application of a statistical model possible. *A priori*, it does not necessarily induce the conventional normalization to unit area (equation (2)). To be consistent with the conventional model, the statistical model must state that each transformed trixel  $y_i$  can be decomposed into its fixed part, corresponding to the linear combination of fundamental functions and spatial distributions of the conventional model, and a residual part, corresponding to the random error. In multivariate analysis, the fixed-effect model (Caussinus 1986) fulfils this condition and includes statistical properties of the error.

#### 3.1. Definition of the fixed-effect model

The fixed-effect model is defined as follows (Caussinus 1986):

- (i) the  $y_i$  are  $N$  independent random vectors defined on a probability space and can be written  $y_i = \tilde{y}_i + \sigma e_i$ , where  $\tilde{y}_i$  is the fixed effect of  $y_i$  and  $\sigma e_i$  is the random error;
- (ii) the expectation of  $y_i$  is  $\tilde{y}_i$ :

$$E(y_i) = \tilde{y}_i$$

that is  $E(e_i) = 0$ ;

- (iii) the variance of  $y_i$  can be written

$$\text{Var}(y_i) = (\sigma^2/\omega_i)\Gamma$$

where  $\Gamma$  is a  $(P, P)$  symmetric positive definite matrix which is known or estimated as well as the positive weights,  $\omega_i$ , associated with  $y_i$ ; and

- (iv) there exists a  $(Q + 1)$ -dimensional linear manifold  $\mathbb{S}$  of  $\mathbb{R}^P$  ( $Q + 1 < P$ ) such that all vectors  $\tilde{y}_i$  belong to  $\mathbb{S}$ .

The linear manifold  $\mathbb{S}$ , the  $N$  vectors  $\tilde{y}_i$  belonging to  $\mathbb{S}$  and the parameter  $\sigma$  have to be estimated.

3.2. Solution of the fixed effect model

The least-squares estimate of  $\mathbb{S}$  is obtained by minimizing

$$\sum_{i=1}^N \omega_i |y_i - \tilde{y}_i|_{\mathbf{M}}^2 \tag{4}$$

where  $\mathbf{M}$  is a  $(P, P)$  symmetric positive definite matrix which defines a metric of  $\mathbb{R}^P$ . It has been shown that the minimum of (4) is reached for  $\mathbb{S}$  such that (Caussinus 1986):

(i) the origin of  $\mathbb{S}$  is  $\bar{y}$ , defined by

$$\bar{y} = \left( 1 / \sum_{i=1}^N \omega_i \right) \sum_{i=1}^N \omega_i y_i$$

and

(ii)  $\mathbb{S}$  is parallel to the subspace of  $\mathbb{R}^P$  spanned by the  $Q$  eigenvectors  $u_q$  associated with the  $Q$  largest eigenvalues  $\lambda_q$  of the matrix  $(\mathbf{Y} - 1_N \bar{\mathbf{Y}})^t \mathbf{D} (\mathbf{Y} - 1_N \bar{\mathbf{Y}}) \mathbf{M}$ , where  $\mathbf{Y}$  is the  $(N, P)$  matrix of the trixels  $y_i$ ,  $\bar{\mathbf{Y}}$  is the  $(1, P)$  matrix of  $\bar{y}$ ,  $1_N$  is an  $(N, 1)$  matrix of ones,  $\mathbf{D}$  is the diagonal  $(N, N)$  matrix of the weights  $\omega_i$  and  $^t$  denotes the transpose.

Consequently,  $\mathbb{S}$  depends on the metric  $\mathbf{M}$ . For small enough  $\sigma$ , the perturbation theory can be used to show that the expectation of (4) is minimized when  $\mathbf{M} = \mathbf{\Gamma}^{-1}$  (Caussinus 1986). Furthermore, when  $N$  is large enough, the same result has also been demonstrated using an asymptotic study (Fine and Pousse 1992).

3.3. Application of the fixed-effect model to FAMIS orthogonal analysis

When the fixed-effect model is applied to the transformed trixels  $y_i$  processed by FAMIS, the effect  $\tilde{y}_i$  represents the relevant part of  $y_i$ , while the noise is assumed to be the random error  $\sigma e_i$ .  $\mathbb{S}$  corresponds to the study subspace in which mainly the relevant part of the trixels is represented, without the noise. In this subspace, the relevant part  $\tilde{y}_i$  of the trixels can be reconstituted using the following formula (Jolliffe 1986):

$$\tilde{y}_i = \bar{y} + \sum_{q=1}^Q \sqrt{\lambda_q} v_q(i) u_q$$

i.e.

$$\bar{\mathbf{Y}} = 1_N \bar{\mathbf{Y}} + \mathbf{V}_Q \mathbf{\Lambda}_Q \mathbf{U}_Q = \mathbf{V} \mathbf{\Lambda} \mathbf{U} \tag{5}$$

with

$$\mathbf{V} = \begin{pmatrix} 1 \\ \vdots \\ \mathbf{v}_Q \\ 1 \end{pmatrix} \quad \mathbf{U} = \begin{pmatrix} \bar{y}_1 & \dots & \bar{y}_P \\ & \mathbf{U}_Q & \end{pmatrix} \quad \mathbf{\Lambda} = \begin{pmatrix} 1 & 0 \\ 0 & \mathbf{\Lambda}_Q \end{pmatrix}.$$

$\mathbf{U}_Q$  is the  $(Q, P)$  matrix composed of the eigenvectors  $u_q$  of  $(\mathbf{Y} - 1_N \bar{\mathbf{Y}})^t \mathbf{D} (\mathbf{Y} - 1_N \bar{\mathbf{Y}}) \mathbf{M}$ ,  $\mathbf{V}_Q$  is the  $(N, Q)$  matrix of the coordinates  $v_q(i)$  of the trixels in the basis  $\{u_q\}_{q=1 \dots Q}$  and  $\mathbf{\Lambda}_Q$  is the  $(Q, Q)$  diagonal matrix whose diagonal elements are the square roots of the eigenvalues  $\lambda_q$ .

$\mathbf{U}_Q$  and  $\mathbf{V}_Q$  satisfy the following relationships (Jolliffe 1986):

$$\mathbf{U}_Q \mathbf{M} \mathbf{U}_Q^t = \mathbf{I}_d \quad \mathbf{V}_Q^t \mathbf{D} \mathbf{V}_Q = \mathbf{I}_d \quad \mathbf{V}_Q = (\mathbf{Y} - 1_N \bar{\mathbf{Y}}) \mathbf{M} \mathbf{U}_Q^t \mathbf{\Lambda}_Q^{-1}.$$

#### 4. FAMIS physical model

The relevant part of the trixels issued from the solution of the statistical model is assumed to follow a physical model.

##### 4.1. Definition of the physical model

The first hypothesis of the conventional FAMIS model is the linear additive decomposition of the relevant part of the transformed trixels (equation (1)). It can be written, in matrix form,

$$\bar{\mathbf{Y}} = \mathbf{A}\mathbf{F} \quad (6)$$

where  $\mathbf{F}$  is the  $(K, P)$  matrix composed of the  $K$  fundamental functions and  $\mathbf{A}$  is the  $(N, K)$  matrix composed of the  $K$  fundamental spatial distributions. The normalization of  $y_i$  and  $f_k$  always leads to a normalization for  $a_k$ . For instance, the conventional unit normalization of  $y_i$  and  $f_k$  (equation (2)) yields

$$\sum_{k=1}^K a_k(i) = 1$$

i.e.

$$\mathbf{A}\mathbf{1}_K = \mathbf{1}_N. \quad (7)$$

The conventional FAMIS model includes two other hypotheses:

(i)  $Q = K - 1$ , that is the number  $K$  of fundamental functions is equal to the dimension of the study subspace minus 1; and

$$(ii) \quad f_k = \bar{y} + \sum_{q=1}^Q t_{kq} u_q \quad (8)$$

i.e., in matrix form,

$$\mathbf{F} = \mathbf{T}\mathbf{U} \quad (9)$$

where  $\mathbf{T}$  is a matrix of dimensions  $(K, Q + 1)$ , i.e.  $(K, K)$ , defined by

$$\mathbf{T} = \begin{pmatrix} 1 & & \\ \vdots & \mathbf{T}_Q & \\ 1 & & \end{pmatrix}$$

and  $\mathbf{T}_Q$  is the  $(K, Q)$  matrix of  $t_{kq}$  coefficients.

This equation states that the fundamental functions belong to the study subspace  $\mathbb{S}$  and that the coordinate of each  $f_k$  on the vector  $\bar{y}$  is equal to one.

#### 4.2. Solution of the physical model: generalization of the oblique analysis

The oblique analysis consists in finding  $\mathbf{T}$ , that is  $K$  factors in a  $(K - 1)$ -dimensional subspace. The most common approach to determine  $\mathbf{T}$  is an iterative apex-seeking procedure (Barber 1980, Di Paola *et al* 1982) taking account for some constraints related to the factors and/or to the factor images. The most frequently used constraints are non-negativity constraints and normalization constraints on both factors and factor images. In order to be consistent with the previous statistical model, we extend the conventional apex-seeking procedure to include the optimal metric used in the orthogonal analysis.

Given an initial estimation of  $\mathbf{T}$  (Barber 1980, Di Paola *et al* 1982),  $\mathbf{A}$  is expressed from  $\mathbf{T}$  using relationships (5), (6) and (9):

$$\tilde{\mathbf{Y}} = \mathbf{A}\mathbf{F} = \mathbf{A}\mathbf{T}\mathbf{U} = \mathbf{V}\mathbf{\Lambda}\mathbf{U}$$

hence

$$\mathbf{A}\mathbf{T} = \mathbf{V}\mathbf{\Lambda}$$

and

$$\mathbf{A} = \mathbf{V}\mathbf{\Lambda}\mathbf{T}^{-1}. \quad (10)$$

Non-negativity constraints are first applied to the  $a_k(i)$  (Barber 1980, Di Paola *et al* 1982) followed by normalization constraints. For instance, if the conventional normalization is used, equation (7) must be satisfied.

Multiplying both sides of equation (10) on the left by  $(\mathbf{V}^t\mathbf{D}\mathbf{V})^{-1}\mathbf{V}^t\mathbf{D}$ , we obtain

$$\mathbf{T}^{-1} = \mathbf{\Lambda}^{-1}(\mathbf{V}^t\mathbf{D}\mathbf{V})^{-1}\mathbf{V}^t\mathbf{D}\mathbf{A}. \quad (11)$$

The matrix  $\mathbf{T}$  corresponding to the modified  $\mathbf{A}$  is computed from (11).  $\mathbf{F}$  is deduced from  $\mathbf{T}$  by equation (9). The  $f_k(j)$  computed values are modified to take non-negativity constraints and normalization constraints (equation (3)) into account. Multiplying both sides of equation (9) on the right by  $\mathbf{M}\mathbf{U}^t(\mathbf{U}\mathbf{M}\mathbf{U}^t)^{-1}$ , we obtain the matrix  $\mathbf{T}$  corresponding to the modified factors

$$\mathbf{T} = \mathbf{F}\mathbf{M}\mathbf{U}^t(\mathbf{U}\mathbf{M}\mathbf{U}^t)^{-1}. \quad (12)$$

$\mathbf{A}$  can then be computed from equation (10) and so on. This procedure is repeated until a stopping criterion is met (for instance the number of negative  $a_k(i)$  values falls below a user-specified value). Figure 1 summarizes this generalized apex-seeking procedure.

##### 0. Initial estimation of $\mathbf{T}$ .

1. Computation of  $\mathbf{A}$  using  $\mathbf{A} = \mathbf{V}\mathbf{\Lambda}\mathbf{T}^{-1}$  (equation (10)).
2. Modification of the  $a_k(i)$  values using non-negativity and normalization constraints related to the  $a_k(i)$  (e.g. equation (7)).
3. Computation of  $\mathbf{T}$  by  $\mathbf{T}^{-1} = \mathbf{\Lambda}^{-1}(\mathbf{V}^t\mathbf{D}\mathbf{V})^{-1}\mathbf{V}^t\mathbf{D}\mathbf{A}$  (equation (11)).
4. Computation of  $\mathbf{F}$  by  $\mathbf{F} = \mathbf{T}\mathbf{U}$  (equation (9)).
5. Modification of the  $f_k(j)$  values using non-negativity and normalization constraints related to the  $f_k(j)$  (e.g. equation (3)).
6. Computation of  $\mathbf{T}$  by  $\mathbf{T} = \mathbf{F}\mathbf{M}\mathbf{U}^t(\mathbf{U}\mathbf{M}\mathbf{U}^t)^{-1}$  (equation (12)).
7. Test of stopping criterion and return to 1 if it is not satisfied.

Figure 1. Generalized apex-seeking procedure.

### 5. Application to scintigraphic data

As FAMIS is primarily used in scintigraphy and the statistical properties of scintigraphic data are well known, we first apply our theoretical approach to this imaging modality.

#### 5.1. Statistical model for scintigraphic data

In scintigraphy, each trixel  $x_i$  corresponds to the realization of  $P$  Poisson distributed variables of parameters  $v_{ij}$  (Barrett and Swindell 1981). An approximate expression of  $v_{ij}$  is  $v_{ij} = v_i.v_j/v_{..}$  (Kendall and Stuart 1967) where

$$v_i = \sum_{j=1}^P v_{ij} \quad v_j = \sum_{i=1}^N v_{ij} \quad \text{and} \quad v_{..} = \sum_{i=1}^N \sum_{j=1}^P v_{ij}.$$

$v_i$ ,  $v_j$  and  $v_{..}$  are unknown. They can be replaced by their maximum likelihood estimators  $x_i$ ,  $x_j$  and  $x_{..}$  respectively, with

$$x_i = \sum_{j=1}^P x_{ij} \quad x_j = \sum_{i=1}^N x_{ij} \quad \text{and} \quad x_{..} = \sum_{i=1}^N \sum_{j=1}^P x_{ij}.$$

To be consistent with the fixed-effect model, the transformation  $g(x_i) = (1/x_i)x_i$  is considered. It follows that

$$E(y_i) = (1/x_i)E(x_i) = (x_{.1}/x_{..}, \dots, x_{.j}/x_{..}, \dots, x_{.P}/x_{..})$$

and

$$\text{Var}(y_i) = (1/x_i^2)\text{Var}(x_i) = \text{diag}(x_{.1}/x_i x_{..}, \dots, x_{.j}/x_i x_{..}, \dots, x_{.P}/x_i x_{..}).$$

#### 5.2. Solution of the statistical model for FAMIS orthogonal analysis

In the framework of the fixed-effect model, we have

$$(\sigma^2/\omega_i)\Gamma = \text{diag}(x_{.1}/x_i x_{..}, \dots, x_{.j}/x_i x_{..}, \dots, x_{.P}/x_i x_{..}).$$

For  $\sigma^2$  to be small, the following identifications are performed:

$$\sigma^2 = 1/x_{..} \quad \omega_i = x_i/x_{..} \quad \text{and} \quad \Gamma = \text{diag}(x_{.1}/x_{..}, \dots, x_{.j}/x_{..}, \dots, x_{.P}/x_{..}).$$

Then, according to the solution of the fixed-effect model, the origin of  $\mathbb{S}$  is  $\bar{y}$  with elements  $\bar{y}_j$  such that

$$\bar{y}_j = \left(1 / \sum_{i=1}^N \omega_i\right) \sum_{i=1}^N \omega_i y_{ij} = \sum_{i=1}^N \frac{x_i x_{ij}}{x_{..} x_i} = \frac{x_{.j}}{x_{..}}.$$

$\mathbb{S}$  is parallel to the subspace of  $\mathbb{R}^P$  spanned by the  $Q$  eigenvectors  $u_q$  associated with the  $Q$  largest eigenvalues  $\lambda_q$  of the matrix  $(Y - 1_N \bar{Y})' D (Y - 1_N \bar{Y}) M$ , with

$$\bar{Y} = (x_{.1}/x_{..}, \dots, x_{.j}/x_{..}, \dots, x_{.P}/x_{..}) \quad D = \text{diag}(x_{.1}/x_{..}, \dots, x_{.i}/x_{..}, \dots, x_{.N}/x_{..})$$

$$M = \Gamma^{-1} = \text{diag}(x_{..}/x_{.1}, \dots, x_{..}/x_{.j}, \dots, x_{..}/x_{.P}).$$

Each element  $(i, j)$  of this matrix is

$$\sum_{k=1}^N \left( \frac{x_{ki} - x_k x_{.i}/x_{..}}{x_k} \right) \left( \frac{x_{kj} - x_k x_{.j}/x_{..}}{x_j} \right).$$

The eigendecomposition of this matrix (Greenacre 1983) corresponds to the eigendecomposition performed in correspondence analysis (Benzecri 1973). Consequently, the optimal orthogonal decomposition to determine the study subspace for scintigraphic data is that used in correspondence analysis.

### 5.3. Solution of the FAMIS physical model by the generalized oblique analysis

The eigenvectors  $u_q$  obtained by correspondence analysis are such that (Benzecri 1973)

$$\bar{Y}MU_Q^t = 0 \quad (13)$$

and we also have

$$\bar{Y}M\bar{Y}^t = 1. \quad (14)$$

Let us compare the FAMIS physical model and the result of the orthogonal decomposition. From the physical model (equations (6) and (8)), it follows that

$$\bar{Y} = AF = A(1_K \bar{Y} + T_Q U_Q).$$

Multiplying both sides on the right by  $M\bar{Y}^t$  and using equations (13) and (14), we obtain

$$\bar{Y}M\bar{Y}^t = A1_K \bar{Y}M\bar{Y}^t + AT_Q U_Q M\bar{Y}^t = A1_K. \quad (15)$$

On the other hand, the orthogonal decomposition is given by equation (5):

$$\bar{Y} = 1_N \bar{Y} + V_Q \Lambda_Q U_Q.$$

Multiplying both sides on the right by  $M\bar{Y}^t$  and using equations (13) and (14), we obtain

$$\bar{Y}M\bar{Y}^t = 1_N \bar{Y}M\bar{Y}^t + V_Q \Lambda_Q U_Q M\bar{Y}^t = 1_N. \quad (16)$$

Equations (15) and (16) lead to

$$A1_K = 1_N.$$

Consequently, when using the orthogonal decomposition of correspondence analysis, the normalization (7) naturally appears, without stating an *a priori* normalization for  $f_k$ . When correspondence analysis is performed, the equations involved in the iterative scheme are simplified. Indeed, since  $U_Q MU_Q^t = Id$  and due to the properties (13) and (14), we have

$$UMU^t = Id.$$

Moreover, in correspondence analysis, we have

$$1_N^t DV_Q = 0$$

and

$$1_N^t D1_N = 1.$$

Hence, as  $V_Q^t DV_Q = Id$ , we get

$$V^t DV = Id.$$

Finally, equations (11) and (12) become respectively

$$T^{-1} = \Lambda^{-1} V^t DA$$

and

$$T = FMU^t.$$

### 6. Practical consequences of using the optimal metric

The influence of the choice of the metric involved in FAMIS is illustrated with a dynamic scintigraphic hepato-biliary study.

#### 6.1. Material and method

A dynamic scintigraphic sequence of 60 <sup>90</sup>Tc<sup>m</sup>-HIDA hepatic images 128 × 128 (each of one second duration) was acquired. Four factor analyses of this sequence were carried out. For each analysis, a 4 × 4 pixel clustering was performed, leading to a set of 1024 trixels, and three fundamental structures were searched for. These four analyses differ in the number of analysed trixels (corresponding to an intensity thresholding) and in the metric used: either the 681 trixels having the higher intensities  $x_i > 11$  or only the 467 trixels such that  $x_i > 1871$  were processed (figure 2); and two choices of metric were investigated:

- (i)  $\bar{y}_j = (1/N) \sum_{i=1}^N y_{ij}$ ,  $\mathbf{M} = \mathbf{Id}$ ,  $\mathbf{D} = (1/N)\mathbf{Id}$ : the orthogonal analysis is the principal component analysis (PCA) performed on centred profiles; and
- (ii)  $\bar{y}_j = x_{j./x_{..}}$ ,  $\mathbf{M} = \text{diag}(x_{..}/x_{.1}, \dots, x_{..}/x_{.j}, \dots, x_{..}/x_{.P})$ ,  $\mathbf{D} = \text{diag}(x_{1.}/x_{..}, \dots, x_{i.}/x_{..}, \dots, x_{N.}/x_{..})$ : the orthogonal analysis is the orthogonal decomposition of correspondence analysis (CA), which is optimal for scintigraphic data.

Combining one thresholding with one metric, the four analyses are denoted PCA/681, CA/681, PCA/467, and CA/467.

#### 6.2. Results

The percentages of data variance associated with the first four eigenvectors are shown in table 1, and the percentages corresponding to the study subspace. The curves in figure 3 represent the cumulated percentages of data variance accounted for by the successive eigenvectors.

Table 1. Percentages of data variance corresponding to the first four eigenvectors, for the scintigraphic dynamic hepatic study. When searching for three factors in FAMIS, the study subspace  $\mathbb{S}$  is parallel to the subspace spanned by  $u_1$  and  $u_2$ .

	$u_1$	$u_2$	$u_3$	$u_4$	$u_1 + u_2$
PCA/681	62.6	4.1	3.6	3.1	66.7
CA/681	77.2	13.9	1.9	0.7	91.1
PCA/467	85.0	6.9	2.3	0.5	91.9
CA/467	76.4	15.9	2.2	0.7	92.3

The factors and associated factor images obtained from the four analyses are displayed in figure 4. The three fundamental structures correspond to: (i) a vascular factor associated with a factor image corresponding essentially to the heart; (ii) a hepatic factor corresponding to the image of the liver; and (iii) an intra-hepatic biliary structure. The contributions  $\text{Contr}(k)$  assigned to every fundamental structure (Di Paola *et al* 1982) are shown in table 2. They are computed from

$$\text{Contr}(k) = \frac{\sum_i \text{Max}(c_k(i), 0)}{\sum_k \sum_i \text{Max}(c_k(i), 0)}$$

where  $c_k(i)$  represents the value of the pixel  $i$  in the factor image  $k$  in the initial spatial sampling

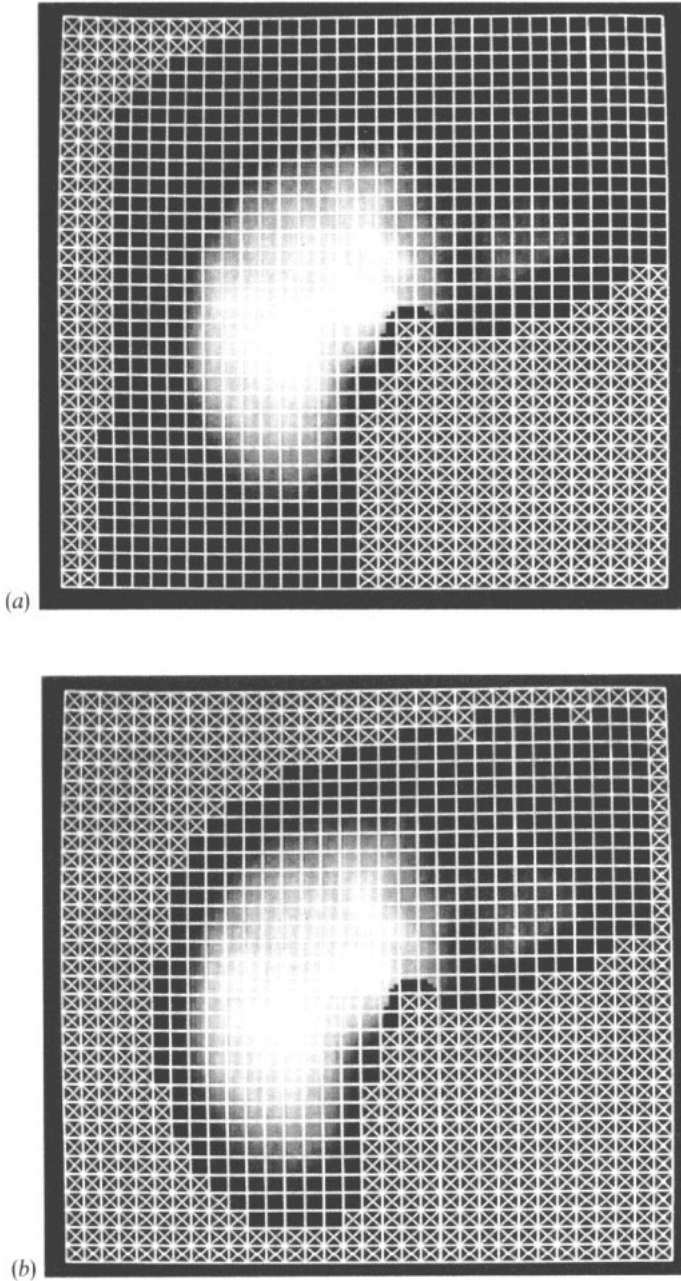


**Figure 2.** (a) Thresholding displayed on the sum image of the 60 dynamic images: the 681 trixels having the higher intensities  $x_i > 11$  were analysed. (b) Thresholding displayed on the sum image of the 60 dynamic images: the 467 trixels having the higher intensities  $x_i > 1871$  were analysed.

### 6.3. Discussion

The sensitivity to the chosen metric appears when there are noisy trixels among the data (681 analysed trixels). In this case, the orthogonal analysis of CA performs a better separation

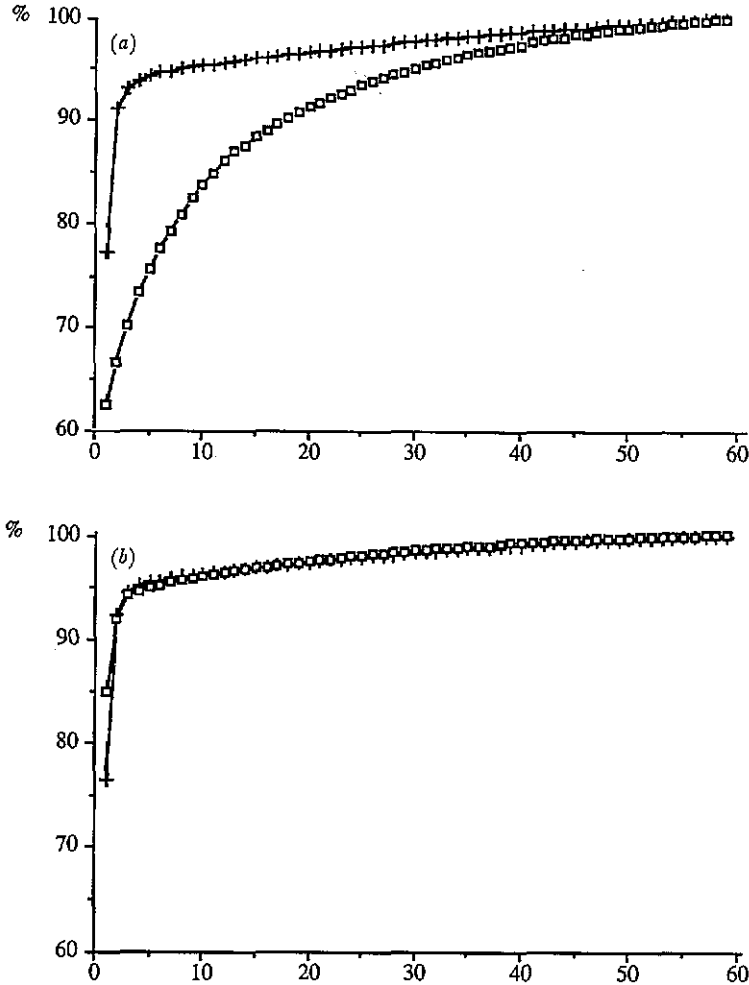


**Figure 3.** Cumulated percentages of data variance accounted for by the successive eigenvectors obtained from principal component analysis ( $\square$ ) and correspondence analysis (+): (a) analyses of the 681 trixels having the higher intensities  $x_i > 11$ ; (b) analyses of the 467 trixels having the higher intensities  $x_i > 1871$ .

between signal and noise: whereas the study subspace describes 66.7% of the data variance when using PCA, 91.1% is represented in the subspace obtained by CA. The curve showing the cumulated percentages of data variance quickly reaches a plateau with CA, but slowly increases with PCA (figure 3). Final results confirm these observations (figure 4): for PCA/681, the factors are noisy. Conversely, the factors issued from CA/681 are relatively smooth. Moreover, the contributions associated with the factor images present noticeable differences (table 2): for instance, the ratio  $\text{Contr}(2)/\text{Contr}(3)$  is about five after PCA/681 and only 2.5 after CA/681.

When the data do not include very noisy trixels (467 analysed trixels), the metric does not play such an important part. The results of the two orthogonal decompositions are similar when considering at least two eigenvectors. The final factors and factor images are also quite similar, as are the contributions. PCA/467 and CA/467 results are close to those

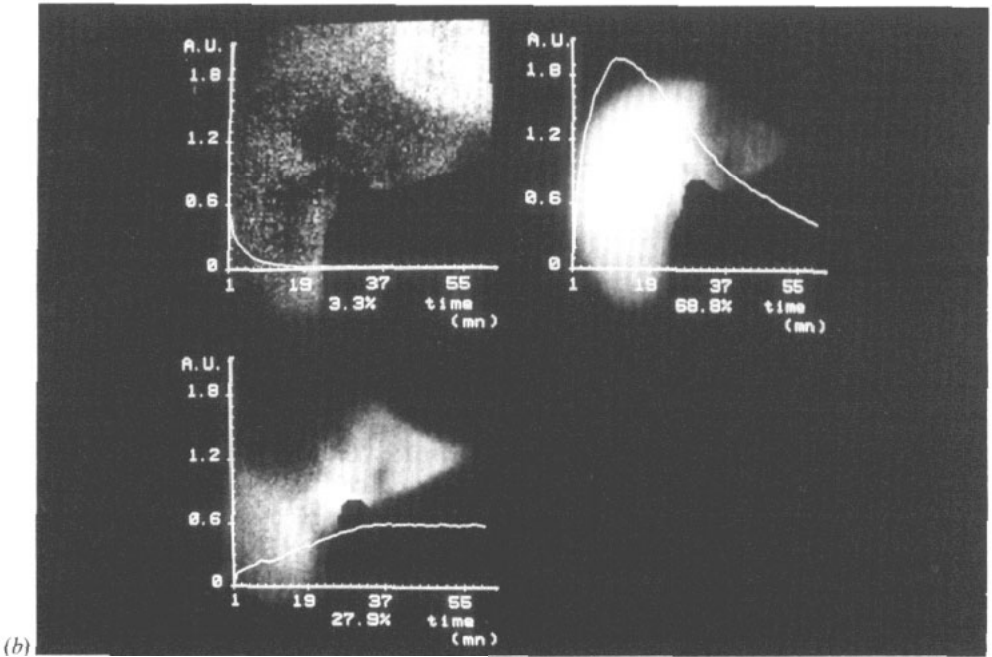
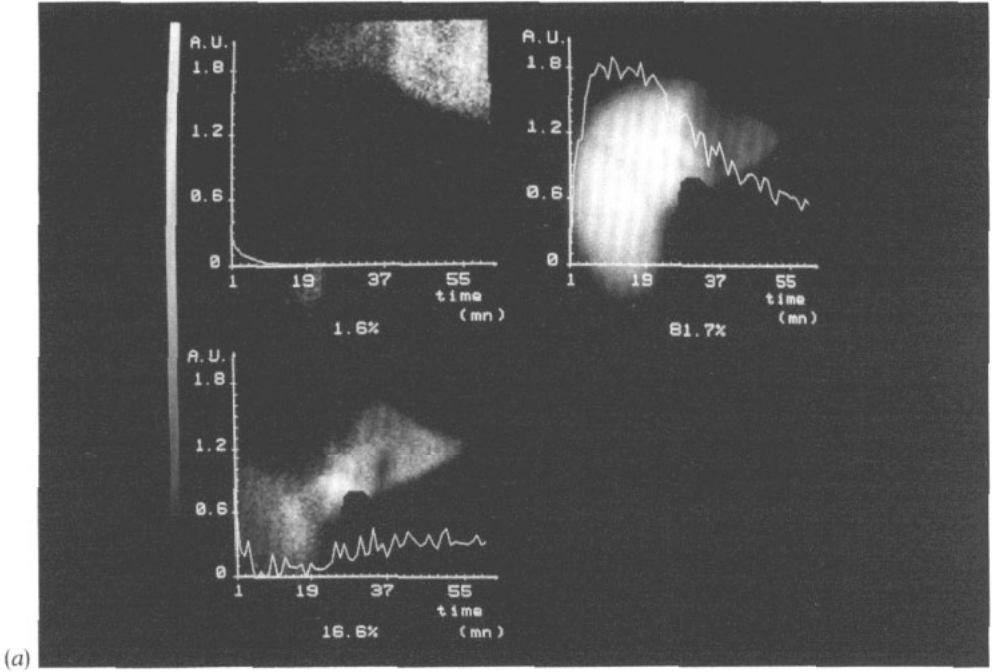


**Figure 4.** FAMIS results: the factors are superimposed on the corresponding factor images. Three fundamental structures were estimated: F1 (top left): vascular structure, F2 (top right): hepatic structure, F3 (bottom left): intra-hepatic biliary structure. (a) PCA/681 results; (b) CA/681 results; (c) PCA/467 results; (d) CA/467 results.

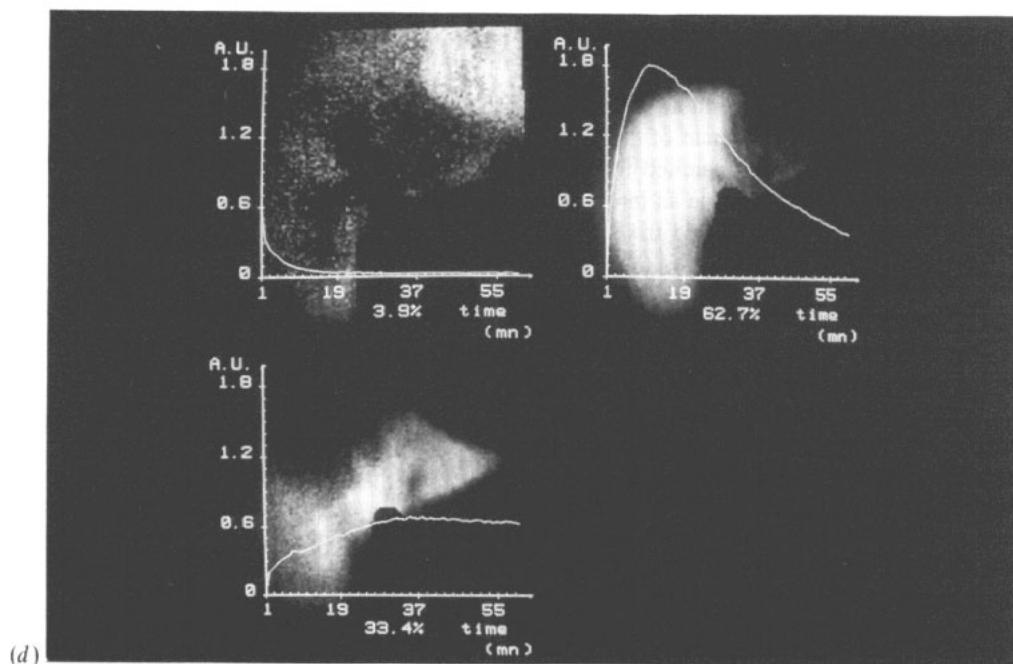
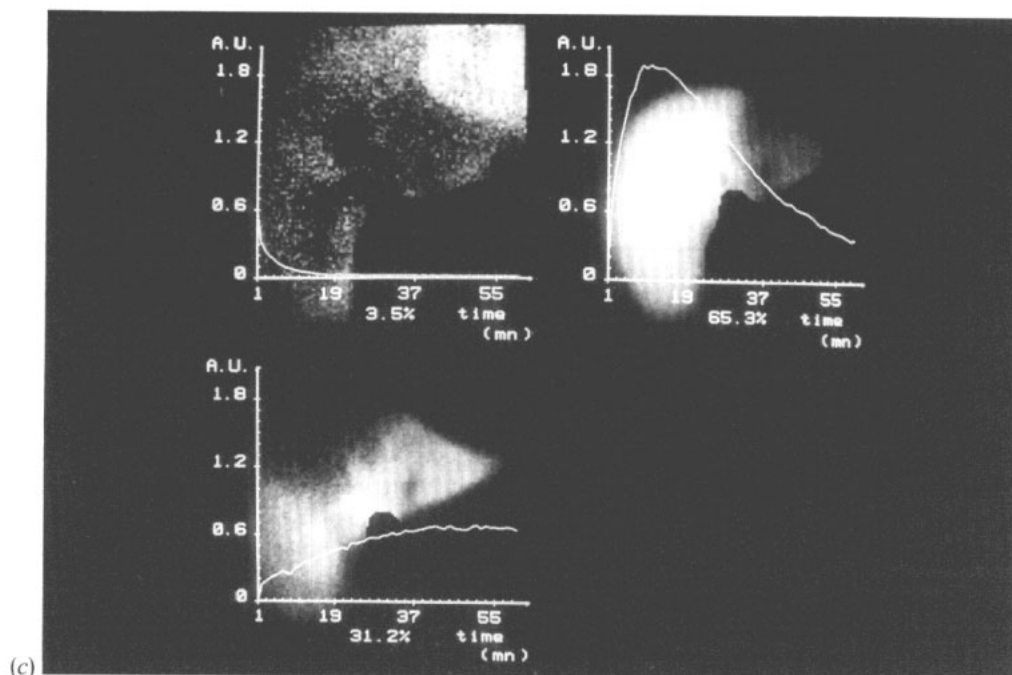


**Table 2.** Percentage contributions associated with the estimated structures for the scintigraphic dynamic hepatic study. Structure 1: vascular structure, structure 2: hepatic structure, structure 3: intra-hepatic biliary structure.

	Structure 1	Structure 2	Structure 3
PCA/681	1.6	81.7	16.6
CA/681	3.3	68.8	27.9
PCA/467	3.5	65.3	31.2
CA/467	3.9	62.7	33.4

obtained with CA/681.

## 7. Discussion

An important stage of FAMIS is the orthogonal decomposition of the data. Its aim is to determine a study subspace in which the whole information underlying the  $N$  trixels is represented, without the noise. 'The problem of whether or not the set of trixels should be normalized in some way is an important issue which has not been properly resolved' (Houston and Nijran 1989). Up to now, various normalizations have been suggested. The most widespread technique consists in performing a PCA of the centred profiles of trixels,  $\mathbf{y}_i - \bar{\mathbf{y}} = (1/x_i)\mathbf{x}_i - (1/N) \sum_{i=1}^N (1/x_i)\mathbf{x}_i$ . The metric is then the identity metric and the same weight  $1/N$  is assigned to every trixel (Barber 1980, Di Paola *et al* 1982). Other methods have also been proposed:

(i) PCA of the raw data,  $\mathbf{x}_i$ , first centred (Gagnon *et al* 1989) or not (Bazin *et al* 1980, Nijran and Barber 1988). In all these cases, the following oblique analysis is not the conventional apex-seeking procedure as described by Barber (1980) and Di Paola *et al* (1982).

(ii) PCA of the profiles without centring (Nijran and Barber 1986). Here, the FAMIS model does not assume the coordinate of the factors on  $\bar{\mathbf{y}}$  to be equal to one in the decomposition (8) and the  $K$  factors are searched for in a  $K$ -dimensional study subspace rather than in a  $(K - 1)$ -dimensional subspace as in conventional FAMIS.

(iii) PCA of the standardized trixels,  $(\mathbf{x}_i - \bar{\mathbf{x}})/s_j$ , where

$$\bar{\mathbf{x}} = \frac{1}{N} \sum_{i=1}^N \mathbf{x}_i \quad s_j = \left[ \frac{1}{N} \sum_{i=1}^N (x_{ij} - \bar{x}_j)^2 \right]^{1/2}.$$

The orthogonal decomposition is thus performed on the correlation matrix (Samal *et al* 1987, 1988). Such a standardization allows the introduction of an original oblique rotation algorithm based on the concept of simple structure (Samal *et al* 1987).

(iv) PCA of normalized trixels  $[1/(\sum_{j=1}^p x_{ij}^2)^{1/2}]\mathbf{x}_i$  (Nakamura *et al* 1989). The determination of the factors and the factor images is based on the maximum-entropy principle and requires the normalization of the trixels. However, the choice of euclidean normalization is not argued.

In the absence of theoretical arguments, practical algorithmic considerations often induce the adopted normalization. In fact, the choice of the metric involved in the eigendecomposition leads to a particular normalization. A theoretical basis for the selection of a metric requires a statistical modelling of the data. Up to now, such a statistical modelling was ignored and only the physical model was considered. The choice of a particular statistical model results from two considerations:

(i) The statistical model must be consistent with the physical one. The fixed-effect model satisfies this requirement since it describes each trixel as the sum of its fixed part and a random part. Referring to the conventional model, the fixed part is identified with the linear combination of the fundamental functions and the spatial distributions.

(ii) The statistical properties of the model must be compatible with the *a priori* knowledge related to the processed data. The fixed-effect model is appropriate to describe the trixels. Indeed, they can reasonably be considered to be independent random vectors since a trixel  $y_i$  cannot be predicted from the observation of any other trixel  $y_{i'}$ , if  $y_i$  and  $y_{i'}$  correspond to any location in the image.

The fixed-effect model requires the variance of the trixels to be known or to be estimated. The statistical properties of the trixels must then be studied. They depend on the imaging modality (scintigraphy, CT, MRI...). In scintigraphy, it is well known that the number of optical photons liberated in a scintillator of an Anger camera can be considered as a Poisson random variable (Barrett and Swindell 1981). As the variance  $v_{ij}$  of a Poisson distributed variable depends on both  $i$  and  $j$ , it is inconsistent with the fixed-effect model.  $v_{ij}$  must then be replaced with an expression where  $i$  and  $j$  are separated. The best first-order approximation of  $v_{ij}$  is  $v_i \cdot v_j / v_{..}$  (Kendall and Stuart 1967) and it makes the fixed-effect model suitable (Caussinus 1986). The variance matrix remains unknown but can be estimated using maximum-likelihood estimators.  $\Gamma$  is then identified and the optimal metric is deduced. It appears that the optimal metric to process scintigraphic data is not the commonly used identity metric, but that corresponding to CA. Furthermore, FAMIS using CA does not require an *a priori* normalization constraint on the factors (equation (3)). It naturally results from the comparison of the FAMIS physical model (equation (6)) with the orthogonal decomposition of the trixels (equation (5)).

To be consistent throughout FAMIS, the optimal metric  $\Gamma^{-1}$  must also be considered during the following oblique analysis. Whereas CA has already been performed for FAMIS orthogonal decomposition without referring to any statistical model (Di Paola *et al* 1976),  $\Gamma^{-1}$  had not previously been introduced in the oblique rotation stage. We show that the conventional apex-seeking procedure can be extended to take  $\Gamma^{-1}$  into account, without losing the advantage of searching for  $K$  factors in a  $(K - 1)$ -dimensional subspace. This feature is attractive from a practical point of view, since the operator can easily visualize and supervise the progress of the analysis, when 2-4 factors are searched (Frouin *et al* 1992). As FAMIS is often used in an interactive way to control the end of the iterative apex-seeking procedure (Frouin *et al* 1992) the search for  $K$  factors in a  $(K - 1)$ -dimensional subspace is convenient.

In scintigraphy, the practical consequences of the use of the optimal metric  $\Gamma^{-1}$  rather than the identity metric appear when processing noisy data. As shown with an example of hepatic study, FAMIS results are less sensitive to the thresholding, that is to the inclusion of noisy trixels among the analysed trixels, when using the  $\Gamma^{-1}$  metric. This greater stability is mainly the consequence of a better separation between signal and noise provided by the orthogonal decomposition. When the processed data do not include very noisy trixels, FAMIS results become similar using either  $\Gamma^{-1}$  or the identity metric.

## 8. Conclusion

The conventional model underlying factor analysis of medical image sequences is revised and split up into a statistical model and a physical one. The introduction of a statistical model allows us to unambiguously determine the optimal metric to be used for the orthogonal

decomposition involved in FAMIS. This metric depends on the expression of the data variance. The conventional apex-seeking procedure solving the oblique analysis of FAMIS is extended to take the optimal metric into account. For scintigraphic data, the variance can be estimated and so the optimal metric is deduced. The optimal orthogonal decomposition is obtained by correspondence analysis.

It is shown by means of a scintigraphic dynamic hepatic study that using the optimal metric makes FAMIS results less sensitive to the inclusion of noisy data and increases the stability of FAMIS results with respect to the choice of the set of analysed trixels.

The determination of the optimal metric for data issued from other imaging modalities requires the study of the statistical properties of the acquired or reconstructed signal. More efficient processing of dynamic MRI, CT, SPECT and PET studies by FAMIS is currently under investigation.

## References

- Barber D C 1980 The use of principal components in the quantitative analysis of gamma camera dynamic studies *Phys. Med. Biol.* **25** 283–92
- Barber D C and Nijran K S 1982 Factor analysis of dynamic radionuclide studies *Proc. 3rd World Congr. of Nuclear Medicine and Biology* vol 1, ed C Raynaud (Paris: WFNMB) pp 31–4
- Barrett H H and Swindell W 1981 The gamma-ray camera *Radiological Imaging—The Theory of Image Formation, Detection, and Processing* (New York: Academic) pp 259–90
- Bazin, J P, Di Paola R, Gibaud B, Rougier P and Tubiana M 1980 Factor analysis of dynamic scintigraphic data as a modelling method. An application to the detection of the metastases *Information Processing in Medical Imaging* ed R Di Paola and E Kahn (Paris: INSERM) pp 345–66
- Benzecri J P 1973 *L'analyse des Données—Tome II: L'analyse des Correspondances* (Paris: Dunod)
- Caussinus H 1986 Models and uses of principal component analysis *Multidimensional Data Analysis* ed J de Leeuw (Leiden: DSWO) pp 149–78
- Di Paola R, Bazin J P, Aubry F, Aurengo A, Cavailloles F, Herry J Y and Kahn E 1982 Handling of dynamic sequences in nuclear medicine *IEEE Trans. Nucl. Sci.* **NS-29** 1310–21
- Di Paola R, Penel C, Bazin J P and Berche C 1976 Factor analysis in scintigraphy *Information Processing in Scintigraphy* ed C Raynaud and A E Todd-Pokropek (Orsay: CEA) pp 91–123
- Fine J and Pousse A 1992 Asymptotic study of functional models, application to the metric choice in Principal Component Analysis *Statistics* **23** 63–83
- Frouin F, Bazin J P, Di Paola M, Jolivet O and Di Paola R 1992 FAMIS: a software package for functional feature extraction from biomedical multidimensional images *Comput. Med. Imag. Graph.* **16** 81–91
- Gagnon D, Todd-Pokropek A, Arsenaault A and Dupras G 1989 Introduction to holospectral imaging in nuclear medicine for scattered subtraction *IEEE Trans. Med. Imaging* **MI-8** 245–50
- Greenacre M J 1983 *Theory and Applications of Correspondence Analysis* (London: Academic)
- Houston A S 1990 Will factor analysis ever become a universally accepted routine in nuclear medicine? *Nucl. Med. Commun.* **11** 401–3
- Houston A S and Nijran K S 1989 Constraint problems in factor analysis of dynamic structures in nuclear medicine *Proc. IEE 3rd Int. Conf. on Image Processing and its Applications* (London: IEE) pp 333–7
- Jolliffe I T 1986 *Principal Component Analysis* (New York: Springer)
- Kendall M G and Stuart A 1967 *The Advanced Theory of Statistics* vol 2 (London: Griffin) p 570
- Nakamura, M, Suzuki Y and Kobayashi S 1989 A method for recovering physiological components from dynamic radionuclide images using the maximum entropy principle: a numerical investigation *IEEE Trans. Biomed. Eng.* **BME-36** 906–17
- Nijran K S and Barber D C 1986 Factor analysis of dynamic function studies using a priori physiological information *Phys. Med. Biol.* **31** 1107–17
- 1988 The importance of constraints in factor analysis of dynamic studies *Information Processing in Medical Imaging* ed C N de Graaf and M A Viergever (New York: Plenum) pp 521–9
- Samal M, Karny M, Surova H, Marikova E and Dienstbier Z 1987 Rotation to simple structure in factor analysis of dynamic radionuclide studies *Phys. Med. Biol.* **32** 371–82
- Samal M, Surova H, Karny M, Marikova E, Penicka P and Dienstbier Z 1988 The reality and meaning of physiological factors *Information Processing in Medical Imaging* ed C De Graaf and M Viergever (New York: Plenum) pp 499–519